



Geophysical Research Letters®

RESEARCH LETTER

10.1029/2021GL094178

Key Points:

- Net transport through Davis and Nares Strait reversed from southward, in December 2010 to northward back toward the Arctic Ocean
- The transport reversal was driven by anomalous winter winds over the Labrador Sea
- The anomalous winds were associated with a record high of the Greenland Blocking Index and a change in the storm track

Supporting Information:

Supporting Information may be found in the online version of this article.

Correspondence to:

P. G. Myers, pmyers@ualberta.ca

Citation:

Myers, P. G., Castro de la Guardia, L., Fu, C., Gillard, L. C., Grivault, N., Hu, X., et al. (2021). Extreme high Greenland Blocking Index leads to the reversal of Davis and Nares Strait net transport toward the Arctic Ocean. *Geophysical Research Letters*, 48, e2021GL094178. https://doi.org/10.1029/2021GL094178

Received 3 MAY 2021 Accepted 6 AUG 2021

Extreme High Greenland Blocking Index Leads to the Reversal of Davis and Nares Strait Net Transport Toward the Arctic Ocean

Paul G. Myers¹, Laura Castro de la Guardia^{1,2}, Chuanshuai Fu¹, Laura C. Gillard^{1,2}, Nathan Grivault¹, Xianmin Hu¹, Craig M. Lee³, G. W. K. Moore⁴, Clark Pennelly¹, Mads Hvid Ribergaard⁵, and Joy Romanski⁶

¹Department of Earth and Atmospheric Sciences, University of Alberta, Edmonton, AB, Canada, ²Center of Earth Observation Science, University of Manitoba, Winnipeg, MB, Canada, ³Applied Physics Laboratory, University of Washington, Seattle, WA, USA, ⁴Department of Physics, University of Toronto, Toronto, ON, Canada, ⁵Centre for Ocean and Ice, Danish Meteorological Institute, Copenhagen, Denmark, ⁶NASA GISS, Columbia University Center for Climate Systems Research, New York, NY, USA

Abstract Baffin Bay exports Arctic Water to the North Atlantic while receiving northward flowing Atlantic Water. Warm Atlantic Water has impacted the retreat of tidewater glaciers draining the Greenland Ice Sheet. Periods of enhanced Atlantic Water transport into Baffin Bay have been observed, but the oceanic processes are still not fully explained. At the end of 2010 the net transport at Davis Strait, the southern gateway to Baffin Bay, reversed from southward to northward for a month, leading to significant northward oceanic heat transport into Baffin Bay. This was associated with an extreme high in the Greenland Blocking Index and a stormtrack path that shifted away from Baffin Bay. Thus fewer cyclones in the Irminger Sea resulted in less frequent northerly winds along the western coast of Greenland, allowing anomalous northward penetration of warm waters, reversing the volume and heat transport at Davis Strait.

Plain Language Summary Baffin Bay exports cold and fresh Arctic Water to the North Atlantic while receiving northward flowing warm and saline Atlantic Water. This warm Atlantic Water has been shown to drive the retreat of tidewater glaciers. Periods of enhanced Atlantic Water transport into Baffin Bay have been observed. The oceanic processes that led to the enhanced transport of these warm waters into Baffin Bay are still not fully explained. Here we show from a combination of observational and model studies that at the end of 2010 the net transport at Davis Strait, the southern gateway to Baffin Bay, reversed from southward to northward for around a month, leading to significant northward oceanic heat transport into Baffin Bay. Anomalous winter winds kept the Atlantic Water on the West Greenland shelf, to propagate north into Baffin Bay instead of entering the interior Labrador Sea. At the same time, a mid-level high pressure system sat over Greenland, efficiently preventing storms from reaching Baffin Bay. Anomalous winds also generated a positive transport signal that propagated cyclonically around Greenland, trapping warm waters on the West Greenland shelf, while also reversing the flow from the Arctic Ocean at Nares Strait.

1. Introduction

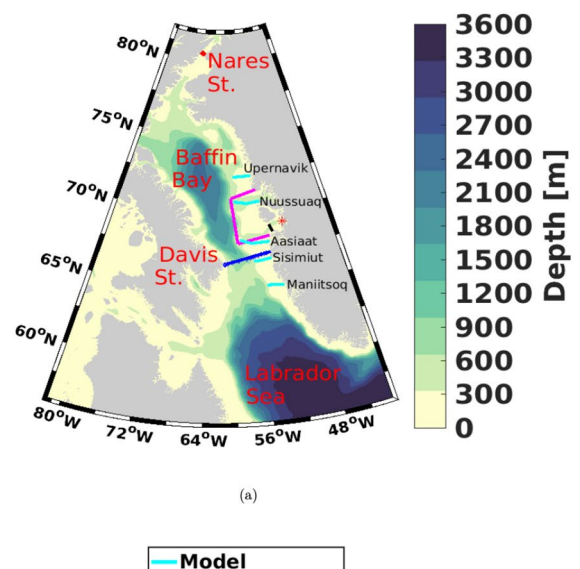
Baffin Bay is a small marginal basin between Greenland and the Canadian Arctic (Figure 1a). It is approximately 550 km east-west and 1,400 km north-south, with broad shelves on the Greenland side and a deep central region (Tang et al., 2004). Based on two distinct periods of mooring observations in 2003–2006 and 2007–2009, net southward fluxes from the Arctic Ocean through Nares Strait were 0.71 ± 0.09 and 1.03 ± 0.11 Sv (Münchow, 2016). Baffin Bay also receives inflow from the Canadian Arctic through Jones Sound $(0.3\pm0.1$ Sv [Melling et al., 2008]) and Lancaster Sound $(0.46\pm0.09$ Sv for 1998–2011 [Peterson et al., 2012]).

At the southern end of Baffin Bay, Davis Strait separates the basin from the Labrador Sea. Davis Strait is wider and deeper than the northern connections and has two-way exchange, with the West Greenland Current (WGC) transporting warm and saline waters of Atlantic origin north into Baffin Bay while the Baffin Island

© 2021. American Geophysical Union. All Rights Reserved.

MYERS ET AL. 1 of 11





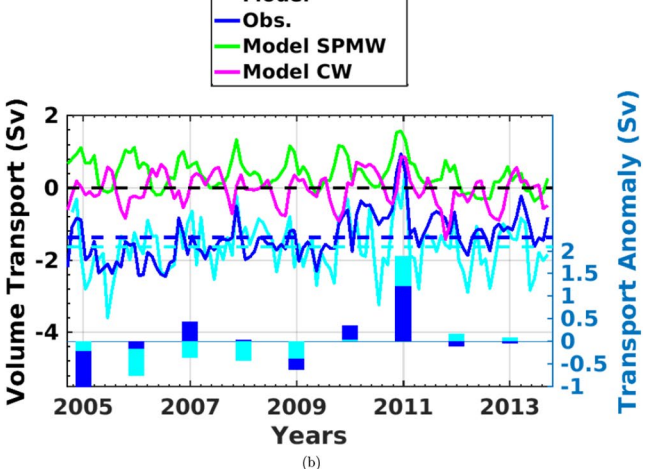


Figure 1. (a) Study region map. Blue diamonds show the observational Davis Strait moorings (Curry et al., 2014). The red line is the Nares Strait section used in the model, consistent with the array of (Münchow, 2016). Five cyan lines show observational Greenland Institute of Natural Resources (GINR) standard sections which were used in the model to show WGC transports (with the model lines extended to the coast). The black line is an additional GINR line across the mouth of Disko Bay, used for extracting of model transports. The red asterisk indicates the location of Jakobshavn Isbrae Glacier. (b) Timeseries of monthly volume transports (in Sv) across Davis Strait, from the observational array (cyan) and the model (blue). The cyan (observational) and blue (model) dashed lines show the mean transports. The black dashed line is the zero transport line. Negative transports indicate southward flow. Model transport for the CW (magenta) and SPMW (green) water masses are shown at the top of the figure using the left scale. The cyan (observational) and blue (model) bars show the anomalous 2-month December-January volume transport (Sv), using the right hand y-axis scale. (c) Mean December-January 2004-2013 mooring based temperatures. (d) December 2010-January 2011 mooring based temperatures. (e) As for panel (c), but for the model. (f) As for panel (d), but for the model. (g) Timeseries of model heat transport (in TW) across Davis Strait. The red dashed line shows the mean heat transport. The black dashed line is the zero transport line. Positive values indicate northward heat transport. The red bars show the anomalous 2-month December-January heat transport, using the right hand scale (TW).

Current transports cold and fresh waters south to the Labrador Sea (Tang et al., 2004). The net volume transport is southward out of Baffin Bay, with the most recent estimate based on continuous measurements over 2004-2010 being 1.6 ± 0.2 Sv (Curry et al., 2014). The global importance of Davis Strait relates to its role in transporting fresher, nutrient-rich and acidic water (Azetsu-Scott et al., 2010, 2012) toward the Labrador Sea where it may impact deep water formation and ecosystems along the coast of North America. The northward flowing WGC brings heat into Baffin Bay which has been linked to the rapid retreat of tidewaters glaciers in West Greenland (Gladish et al., 2015; Holland et al., 2008; Myers & Ribergaard, 2013; Straneo et al., 2012).

The year 2010 was an unusual year in the region. There were record surface air temperatures in SW Greenland (Cappelen, 2018). Mortensen et al. (2018) observed record warm waters inside Godthaabsfjord, which they linked to local atmospheric forcing, produced by a weak winter and a relatively long, warm summer. Cold anomalies, associated with enhanced southward transport of Arctic waters through Davis Strait have been observed in recent years (Mortensen et al., 2018; Rysgaard et al., 2020). Here we show that at the end of 2010 an extremely anomalous large-scale regional atmospheric circulation produced a reversal of the net transport through Baffin Bay toward the Arctic Ocean. This led to significant northward oceanic heat transport into Baffin Bay.

2. Data and Methods

We use daily and monthly objective analysis results for the Davis Strait array, as well as timeseries of transports (Curry et al., 2014). Winds were taken from the ERA5 reanalysis (Hersbach & Dee, 2016; Hersbach et al., 2020). Ekman transports were calculated from December and January daily zonal (τ_x) and meridional (τ_y) windstress over 2004 to 2013, as $M_x = \frac{\tau_y}{\rho f}$ and $M_y = -\frac{\tau_x}{\rho f}$, where f is the Coriolis parameter. Heat transports are computed using a reference temperature of 0°C. Freshwater transport is computed using a reference salinity of 34.8. The choice of reference values for heat and freshwater transport is to be consistent with past studies (Cuny et al., 2005; Curry et al., 2011). Monthly Arctic and North Atlantic Oscillation indices were taken from the Climate Prediction Center (http://www.cpc.ncep.noaa.gov/products/precip/CWlink/ daily_ao_index/teleconnections.shtml) and daily values of the Greenland Blocking Index (GBI) were downloaded from the Physical Sciences Laboratory (http://psl.noaa.gov/data/timeseries/daily/GBI/). The cyclone data set is from the Modeling, Analysis, and Prediction Climatology of Mid-latitude Storminess (Bauer et al., 2016), applied to MERRA2 sea level pressure (Gelaro et al., 2017).

The model used is the Nucleus for European Modeling of the Ocean (NEMO) numerical framework version 3.4 (Madec, 2008). The model is coupled with the Louvain-la-Neuve sea ice model (LIM2) (Fichefet & Morales Maqueda, 1997). The configuration used is called Arctic and Northern Hemisphere Atlantic (ANHA) with a $\frac{1}{12}\,^{\circ}$ resolution (ANHA12). The simulation has an integration time from January 1, 2002 to December 31, 2019. The horizontal resolution ranges from 6.0 km in the Labrador Sea to 4.0 km in northern Baffin Bay (Hu et al., 2018). The atmospheric forcing data used in ANHA12 comes from the Canadian Meteorological

MYERS ET AL. 2 of 11



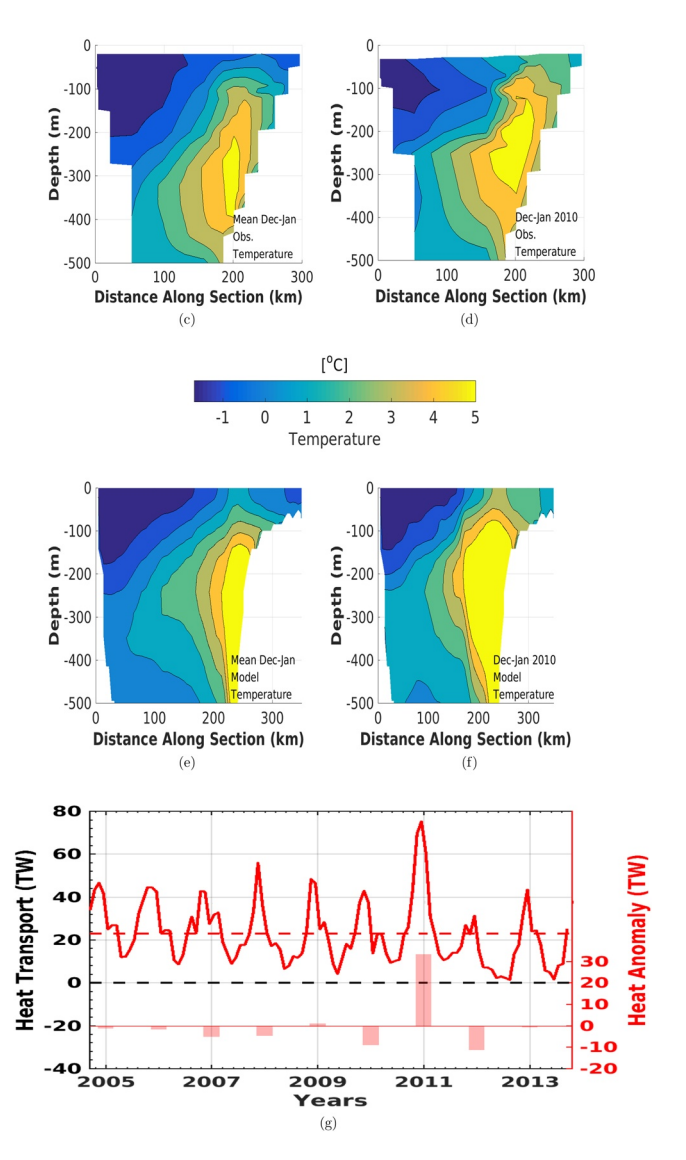


Figure 1. Continued.

Center's Global Deterministic Prediction System (Smith et al., 2014). Further details can be found in Hu et al. (2018).

3. The Signal at Davis Strait in December 2010

We present the observational transport timeseries at Davis Strait, extended from 2010 as originally in Curry et al. (2014) through to the fall of 2013 (Figure 1b). The extension of the timeseries by 3 years does not change the mean from Curry et al. (2014), which remains -1.6 Sv. As in Curry et al. (2014), variability can be seen in the transport at multiple frequencies. One event stands out in the monthly averaged timeseries at the end of 2010, when the December averaged net transports switches to 0.5 Sv northward. To show how unusual this event is, we compute the anomaly of the net Davis Strait transport averaged over a 2 month period of each December–January between 2004 and 2013. Although weaker northward anomalies can be seen (Figure 1b) in the winters of 2006–2007 and 2009–2010, in 2010–2011 the northward anomaly is 1.2 Sv, enough to flip the sign of the net transport to the north in December 2010.

Consistent with Curry et al. (2014), a contour plot of the potential temperature from the moorings, averaged over each December–January between 2004 and 2013, shows cold Arctic water on the west of the section and the warm Atlantic Water core at around 300 m on the eastern side (Figure 1c). Meanwhile, in December–January 2010, the same mooring data shows (Figure 1d) an increase in the area with warm waters, with the core higher up in the water column, between 100 and 200 m.

To help understand this event given the limited amount of winter data in the region, we use model output from ANHA12. Model output is consistent with, and reproduces the event seen in the observations at Davis Strait. The net model transport at Davis Strait, over the same 2004–2013 period, is slightly smaller than the observations, at -1.4 Sv (Figure 1b). The correlation between the model and observed monthly net transport is 0.54, significant at the 99% level. The model represents the same event at the end of 2010, with a northward anomaly of 1.9 Sv in December 2010/January 2011 (Figure 1b).

The model mean December–January temperature across the observational section shows similar structure (Figure 1e). In December 2010/January 2011, consistent with the observations, the warm core in the model covers

a larger area, and is higher in the water column (Figure 1f). The model mean heat transport into Baffin Bay through Davis Strait is 23.0 TW (Figure 1g), consistent with estimates of 18 ± 17 TW between 1987 and 1990 (Cuny et al., 2005) and 20 ± 9 TW over 2004–2005 (Curry et al., 2011). The timing of the maximum in net heat transport in late fall agrees with Cuny et al. (2005) and Curry et al. (2011). The event at the end of 2010 stands out clearly in this timeseries, reaching a peak of 75.3 TW. This event is unique over our decadal record, with a monthly anomaly of 33.2 TW (Figure 1g). The normal export of freshwater from Baffin Bay is also reduced during this event (Figure S1a).

The model also allows us to breakdown the transport by watermass. We use a slightly modified classification to that proposed by Rysgaard et al. (2020) that considers three major water masses in the vicinity of Davis Strait: Baffin Bay Polar Water (BBPW; $\theta \le -1^{\circ}C$; $S \le 33.7$), southwest Greenland Coastal Water (CW; $\theta \ge -1^{\circ}C$; $S \le 34.1$) and subpolar Mode Water (SPMW; $\theta > 2^{\circ}C$; S > 34.1)—a warm saline water of Atlantic origin. Timeseries of model SPMW transport shows (Figure 1b) largest northward transport in the fall, with a peak of 1.6 Sv at the end of 2010. CW transport typically peaks in the summer, including a broad peak of 0.6 Sv northward in the summer of 2010 (Mortensen et al., 2018), but also a peak of 0.9 Sv at the end

MYERS ET AL. 3 of 11



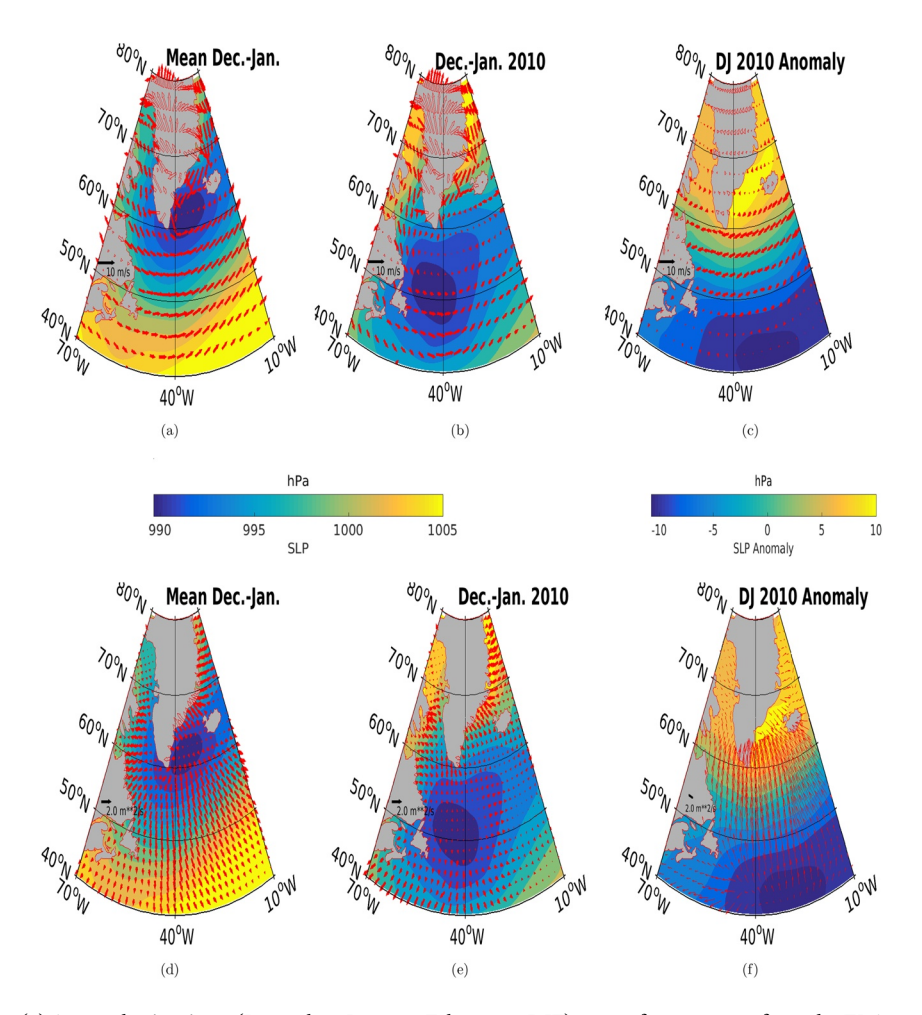


Figure 2. (a) Atmospheric winter (December, January, February—DJF) sea surface pressure from the ERA5 reanalysis, averaged over 1980–2018 with superimposed surface winds over the same time period. (b) As for a, but for the winter of 2010 (December 2010 to February 2011). (c) Sea surface pressure anomaly for winter 2010 compared to the average over the winters 1980–2018, with anomalous wind vectors. (d–f) As in panels (a–c), but with the computed Ekman transport vectors instead of wind vectors. In all vector plots, every fifth vector is plotted to avoid clutter.

of 2010. No signal is seen in the southward flowing BBPW at the end of 2010 (Figure S1b). Similar results can also be seen using other water mass definitions, such as Curry et al. (2014) (Figure S2).

4. Upstream Changes in the Labrador Sea

Given that the temperature and transport anomalies are observed at the eastern side of Davis Strait, in the WGC, we look upstream into the Labrador Sea to explain the enhanced northward transport of warm water masses at Davis Strait. Two-monthly composites of the large-scale winds over the Labrador Sea in winter show that they are cyclonic (Figure 2a), from the northwest, with south and eastward components. They are also the strongest in winter (Schulze Chretien & Frajka-Williams, 2018). However, the same 2 month composites for the end of 2010 shows a different pattern (Figure 2b), with the low pressure shifted to the south, leading to winds more from the north, without a component toward the east near the west coast of Greenland. Thus there is an anomalous wind component from the east during this period at the end of 2010 (Figure 2c).

The normal winter wind situation leads to Ekman transports in the northern Labrador Sea directed from the northeast to the southwest (Schulze Chretien & Frajka-Williams, 2018), supporting offshore exchange from the WGC into the interior of the Labrador Sea (Luo et al., 2016; Schulze Chretien and Frajka-Williams, 2018) (Figure 2d). Given the changed winds at the end of 2010, the Ekman transports differ during

MYERS ET AL. 4 of 11



that 2-month period (Figure 2e), with components to the north and west. Thus the Ekman transport anomalies are directed onshore, toward the WGC (Figure 2f). Although eddies and rings can still exchange water offshore from the WGC (de Jong et al., 2016), the onshore Ekman transport leads to most of the shelf and slope waters remaining near the coast. Without this offshore exchange into the Labrador Sea, there is enhanced northward transport of volume and heat (Figures 3a and 3b), as well as freshwater (Figures S3a and S3b) in the WGC south of Davis Strait.

Using 2 years of observations from the outer part of the Godthaabsfjord system Mortensen et al. (2013) noted that the highest temperatures observed over 2009–2010, above 3°C, were seen at intermediate depths at the end of 2010. An extended timeseries (Mortensen et al., 2018) shows that the water in the outer sill region of Godthaabsfjord was warmest in fall/winter of 2010 in comparison to the rest of the 2006–2016 timeseries. The highest salinity within the actual fjord was recorded the following spring, in May 2011.

5. Baffin Bay Impacts

Continuing northward into Baffin Bay, the same anomalous enhanced transport of volume and heat (Figures 3c–3e), as well as freshwater (Figures S3c–S3e) is seen at the end of 2010 along the WGC. At these three sections, the winter 2010–2011 volume and heat transport anomalies reach 0.9, 1.4 and 0.8 Sv, and 21.1, 23.8 and 7.1 TW, respectively. Effectively, there is an enhanced transport of warm water, rather than a significant increase in the temperature of the inflowing waters. Although the volume transport into Disko Bay in the winter of 2010–2011 is not anomalously large compared to other winters (0.1 Sv), the winter heat transport anomaly is larger than any other winter by over 1.1 TW, and 1.6 TW larger than the 2004–2013 winter mean (Figure 3f). The heat transport into Disko Bay also peaks earlier in the model timeseries, but only in summer, not in the winter.

Focusing on Disko Bay, the model heat content in the top 500 m of the water column peaks at over 400 PJ at the end of 2010 (Figure 4a). After the cold winter of 2010, Joughin et al. (2020) reported the warmest temperatures observed since 1980 at 250 m in Disko Bay in 2011. Gladish et al. (2015) also stated that in the summer of 2011, "warmer than ever" waters filled Disko Bay, as well as being observed on the West Greenland outer shelf. In the following two summers (2012 and 2013), Khazendar et al. (2019) reported the fastest flow speeds for Jacobshavn Isbrae, which is the tidewater glacier with Greenland's largest volume discharge, into Disko Bay.

Compared to a normal December–January time period (Figure 4a), additional heat can be seen extending north from Disko Bay along the coast of Greenland into Melville Bay (Figure 4b). The associated heat content anomaly (Figure 4c) clearly shows the significant warming occurring in the Upernavik region as well as into Melville Bay. In Melville Bay, increases in ice front speed and ice front retreat were seen at multiple glaciers following 2011 (Wood et al., 2018). Compared to farther south along the Greenland coast, a weak signal (approx. 100 PJ) of warming is seen in the Smith Sound region, where two key tidewaters glaciers with the largest discharge in the Canadian Arctic can be found. Enhanced warming and northward volume transport impacts the sea surface height along the west coast of Greenland (Figure 4d). Raised sea levels of at least 0.05 m can be seen all along the coast of Greenland, extending north through Nares Strait and along the north coast of Greenland in the Arctic Ocean.

The propagation of the SSH anomaly leads to a flip in the direction of the net transport at Nares Strait reaching a net of 0.64 Sv northwards in January 2011, compared to the 2004–2013 mean of -0.81 Sv southward (Figure 4e). During this event, the sign of the heat transport switches to -1.3 TW. The freshwater transport reverses direction (Figure S4). The winter 2010–2011 event cannot be seen propagating back south along the western side of Baffin Bay, nor is there a noticeable signal in the transports flowing into Baffin Bay through Barrow Strait/Lancaster Sound.

6. Discussion

To further understand the anomalous oceanographic transport signal, we looked into the atmospheric conditions during this period. We first consider the Greenland Blocking Index (GBI) of Hanna et al. (2016), which has previously been used to explain the extreme melting event of summer 2013 over Greenland

MYERS ET AL. 5 of 11

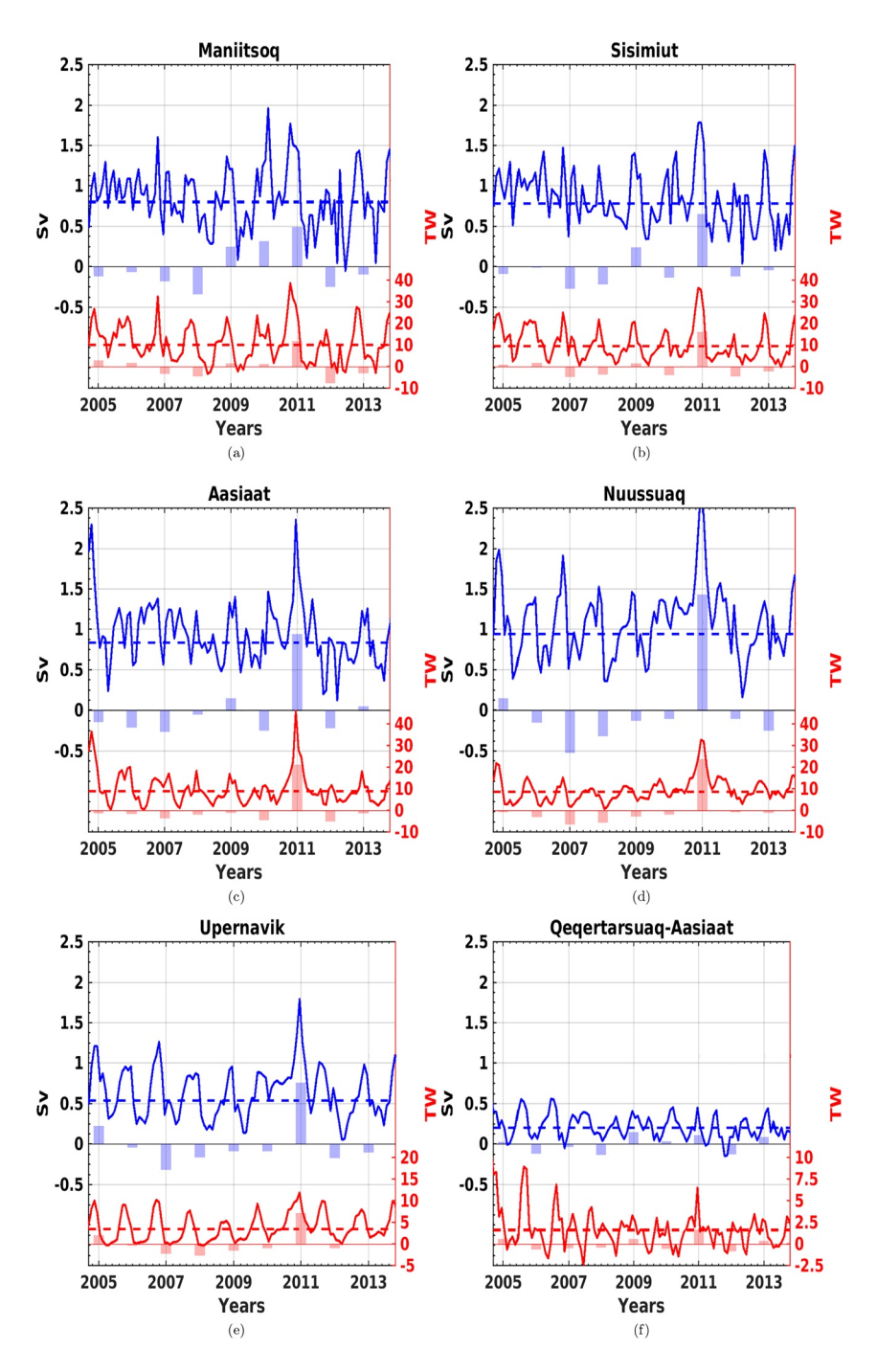


Figure 3. Model transports across West Greenland Current/Disko Bay sections. The blue lines are the volume transport (left scale in Sv) and red lines heat transport (right scale, in TW). The blue dashed line is the mean volume transport and the red dashed line is the mean heat transport. The bars show the anomalous volume (blue, left scale) and heat (red, right scale) transport for the 2-month December–January period compared to the mean of all December–January over 2004–2013. Positive values are northward for panels (a–e), and eastward (into Disko Bay) in panel (f).

(Ballinger et al., 2018; Hanna et al., 2014). The GBI is defined as the mean height of the 500 hPa surface averaged over 60°-80°N, 280°-340°E. The GBI has a maximum over the last 70 years, 3 standard deviations above the mean in the winter of 2010–2011 (Figure 5a). High GBI is associated with warm and wet conditions around Greenland (Hanna et al., 2016). The effects of anomalous GBI extend beyond the icesheet, with the storm track shifted southward, and more toward Europe (Figures 5b and 5c). From composite analysis

MYERS ET AL. 6 of 11



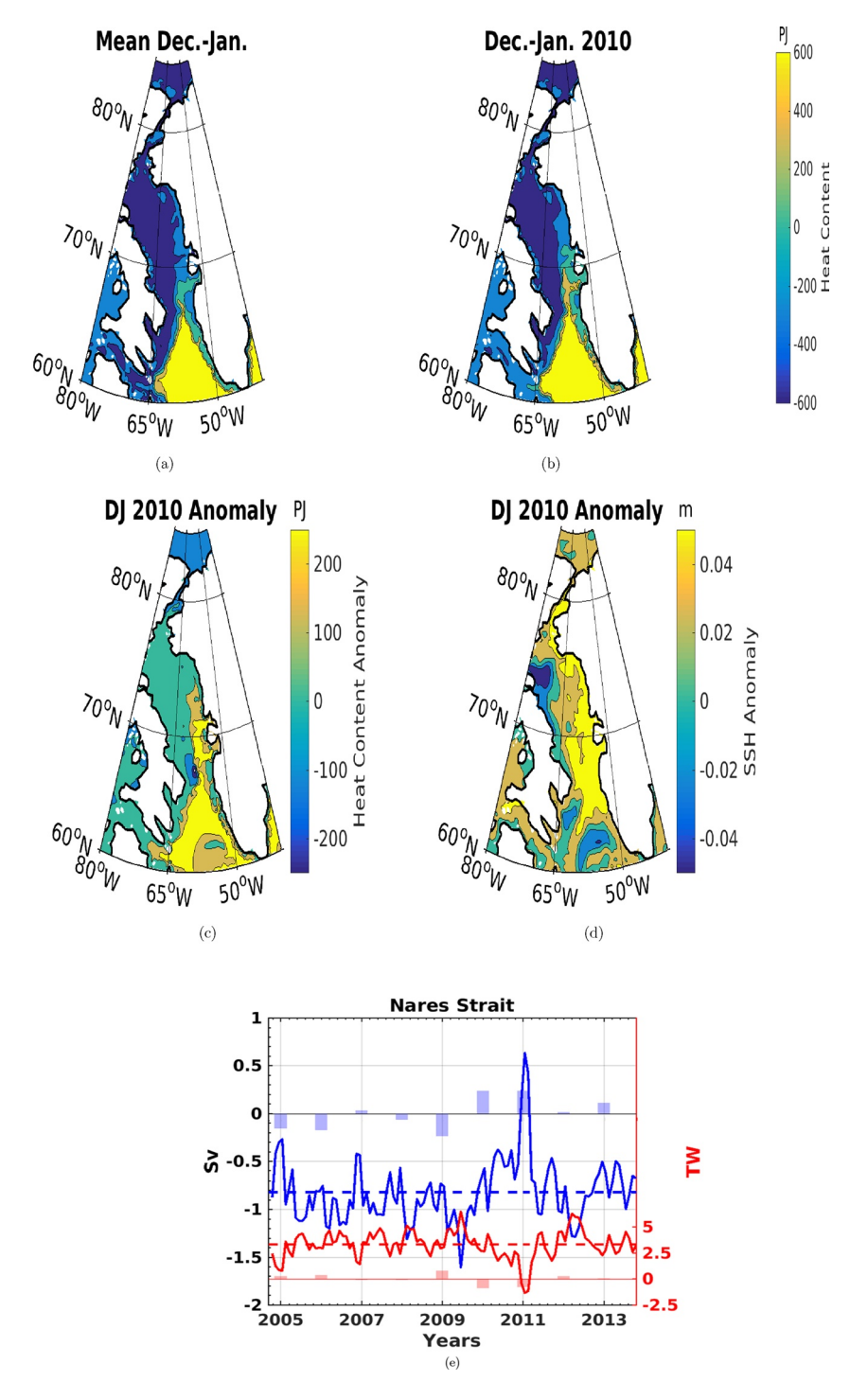


Figure 4. Top 500 m (a) model mean 2004–2013 2-month December–January (DJ) heat content (PJ); (b) model December 2010–January 2011 heat content; (c) Anomalous top 500 m heat content (DJ 2010–2011—DJ 2004–2013). (d) Model sea surface height (SSH) anomaly, for DJ 2010–2011 minus mean DJ 2004–2014. Units in m. (e) The blue line is the model Nares Strait volume transport (left *y*-axis in Sv) and red line is the heat transport (right scale, in TW). The blue dashed line is the mean volume transport and the red dashed line is the mean heat transport. The bars show the anomalous volume (blue, left scale) and heat (red, right scale) transport for the 2-month December–January period compared to the mean of all December–January over 2004–2013. Positive values are northward toward the Arctic Ocean.

MYERS ET AL. 7 of 11



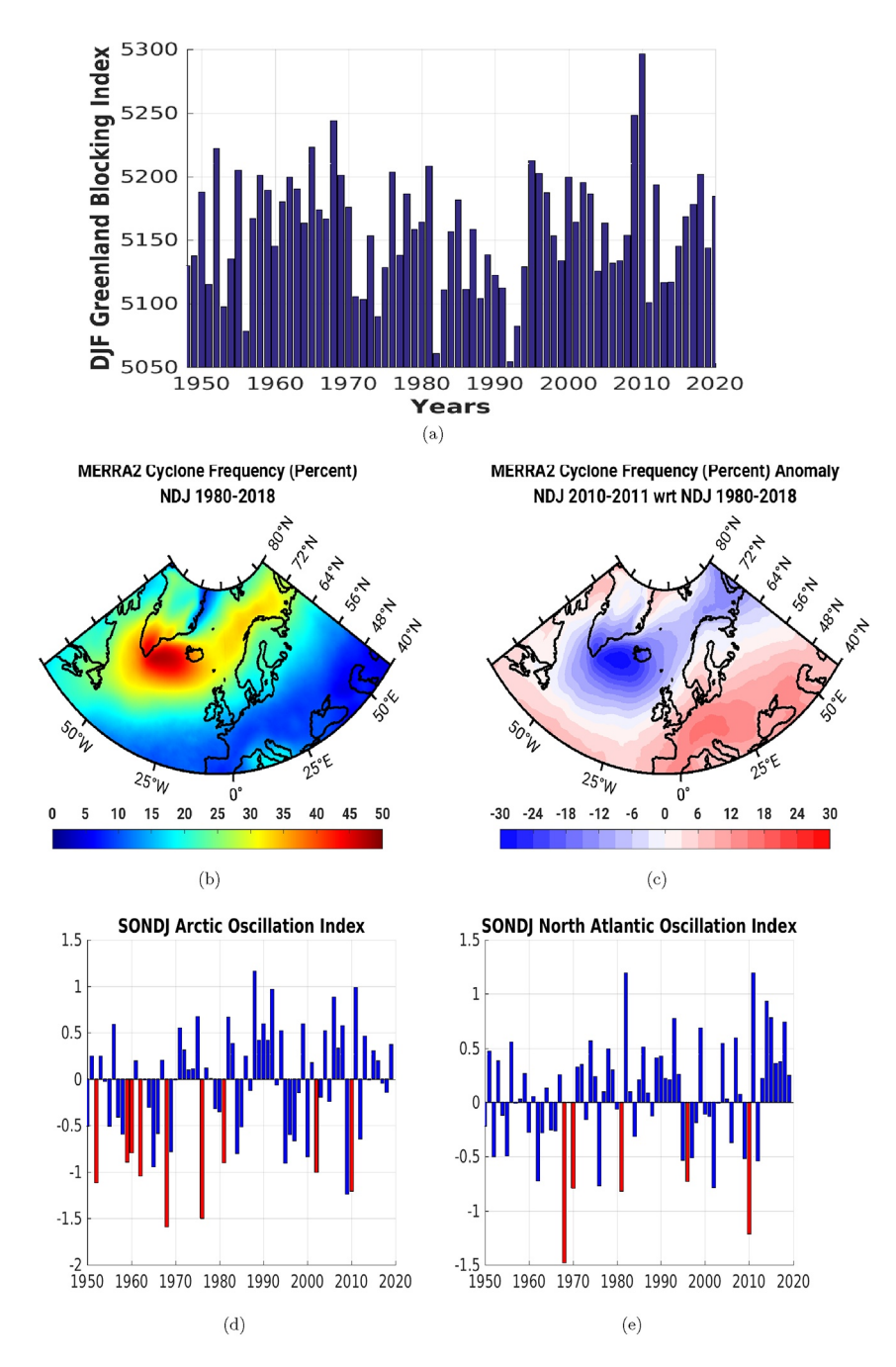


Figure 5. (a) Timeseries of the Greenland Blocking Index (DJF) 1948–2020, in m. (b) Cyclone frequency, in percent, for winter (NDJ) 1980–2018 and (c) for 2010–2011 compared to the 1980–2018 mean. (d) Timeseries of monthly AO, averaged over September, October, November, and December of the given year, plus the following January. Bars shaded red indicate that all monthly values over the 5 month averaging period are negative. Blue bars have one or more months with a positive index through the averaging period. (e) As for panel (d) but for the monthly North Atlantic Oscillation.

of winds during times when there are storms in the Irminger Sea, such storms result in northerly winds along the western coast of Greenland. During the winter of 2010–2011, fewer cyclones in the Irminger Sea resulted in less frequent northerly winds along the western coast of Greenland, allowing anomalous northward penetration of warm waters. We additionally note that the GBI index (Figure 5a) links a low GBI with observed cold periods of the late-1960s/early 1970s, 1982–1984, 1989–1994. Similarly, the period from the 1950s to the mid-1960s is in general warm, and with a high GBI. Noticeable is the change in the mid-1990s

MYERS ET AL. 8 of 11



from a long period of low GBI/cold conditions to high GBI/warm conditions, which started the acceleration of bottom melting of tidewater glaciers for example, Jakobshavn Isbrae since 1997.

We also consider the work of Joyce and Proshutinsky (2007), who applied Godfrey (1989)'s Island Rule to Greenland and the Arctic Ocean. Using NCAR/NCEP reanalysis winds, an estimate of 1 Sv for the Bering Strait inflow and a simple linear representation of friction, Joyce and Proshutinsky (2007) calculated the southward transport through Davis Strait as -2.5 Sv. Using the same model, and winds associated with a low phase of the Arctic Oscillation, Joyce and Proshutinsky (2007) showed that the transport west of Greenland, through Davis Strait (and also Nares Strait, even if it wasn't explicitly stated), could reverse direction. Although Joyce and Proshutinsky (2007) did not examine the time dependent solution, they found that steady state was approached within 3 months.

The monthly Arctic Oscillation (AO) Index values for September 2010 through to January 2011 are -0.865, -0.467, -0.376, -1.749 and -1.683; the 5 month average is -1.2 (Figure 5d). Thus there is a sufficient period with strong negative values of the AO in the autumn of 2010 to spin-up a clockwise circulation around Greenland, leading to the reversal at Davis and Nares Straits. The only other years in the CPC record where these 5 months have negative Arctic Oscillation indices are 1952, 1959 (although December only -0.042), 1960, 1962 (although September -0.056, October -0.016), 1968, 1976 (November -0.087), 1981, and 2002 (September -0.043). Unfortunately we do not have observational data from Davis or Nares Strait region for those winters.

If we repeat the same analysis with the North Atlantic Oscillation (NAO) index, we see again that autumn of 2010 stands out (Figure 5e). Fewer years are highlighted, nor is 2002. Interestingly, 1996 is now highlighted, with 5 consecutive months of negative NAO index. This is significant as it is between 1996 and 1997 that Holland et al. (2008) first identified the presence of Atlantic warm water on the West Greenland shelf and in Disko Bay, impacting Jakobshavn Isbrae. Holland et al. (2008) argued that a change in the sign of the NAO in the winter of 1995–1996 led to a weaker subpolar gyre system, allowing warm SPMW to spread westward, although more recent papers do not support the dominant control of the sub-polar gyre by the NAO (Foukal & Lozier, 2017; Straneo & Heimbach, 2013).

Finally, we note that the anomalous atmospheric conditions reported here might be part of a larger hemispheric signal, given that the winter of 2010–2011 was one of the coldest in the United Kingdom on record (Moore & Renfrew, 2011). Moore and Renfrew (2011) argued the interplay between the NAO and the East Atlantic pattern contributed to the cold, but we now know that in additional to the record GBI, the winter was associated with a sudden stratospheric warming (SSW) and unprecedented Arctic Ozone loss (Manney et al., 2011). Moore et al. (2018) show that the surface response to SSWs looks like the negative phase of the NAO. Thus, to conclude, during the winter of 2010–2011, fewer cyclones in the Irminger Sea resulted in less frequent northerly winds along the western coast of Greenland, allowing anomalous northward penetration of warm waters. In combination with the spin-up of a local wind-driven cyclonic circulation around Greenland, the volume and heat transport is reversed at Davis Strait for one to two months. Going forward, Hanna et al. (2016) stated the greater variability in December GBI, including recent December extreme GBI events, is linked to more positive GBI on average and the negative trend in the NAO since 2000 (Hanna et al., 2015).

Data Availability Statement

Daily and monthly objective analysis results for the Davis Strait array are available online for download (at http://iop.apl.washington.edu/data.html), with the timeseries also available the NSF Arctic Data Center (https://arcticdata.io/catalog/view/doi:10.18739%2FA2G15TB81, https://arcticdata.io/catalog/view/doi:10.18739%2FA2S91S), the repository for US Arctic Observing Network data. The ERA5 data was obtained from ECMWF (https://www.ecmwf.int/en/forecasts/datasets/reanalysis-datasets/era5). Monthly Arctic and North Atlantic Oscillation indices were taken from the Climate Prediction Centre of NOAA (www.cpc.ncep.noaa.gov). Daily values of the Greenland Blocking Index (GBI) were downloaded from https://psl.noaa.gov/data/timeseries/daily/GBI/.

MYERS ET AL. 9 of 11



Acknowledgments

The authors gratefully acknowledge the financial and logistic support of grants from the Natural Sciences and Engineering Research Council (NSERC) of Canada. These includes a Discovery Grant (rgpin227438-09) awarded to P.G. Myers, and a Climate Change and Atmospheric Research Grant (VITALS-RGPCC 433898). The authors are grateful to the NEMO development team and the Drakkar project for providing the model and continuous guidance. The authors would also like to thank G. Smith for the model atmospheric forcing fields, made available by Environment and Climate Change Canada (http://weather.gc.ca/ grib/grib2_glb_25km_e.html). The authors thank Westgrid and Compute Canada for computational resources, where all model experiments were performed. The model code based on the NEMO model is available at https:// www.nemo-ocean.eu/ (last access: May 28, 2017, Madec, 2008). Details on the ANHA configuration used are available at http://knossos.eas.ualberta.ca/anha/ index.php (last access: September 8, 2017), with files for the experiment used in this paper at https://doi. org/10.7939/DVN/GIXGXB (Hu, 2020). Summer internship funding was also provided by University of Alberta International. CML and the Davis Strait Observing System are supported by the US National Science Foundation Arctic Observing Network program under grants OPP1902595, ARC1022472, ARC0632231, and OPP0230381. Mads Hvid Ribergaard was funded by the Danish State through the National Centre for Climate Research. The authors thank two anonymous reviewers for their thoughtful and constructive reviews that led to a significantly improved final manuscript.

References

Azetsu-Scott, K., Clarke, A., Falkner, K., Hamilton, J., Jones, E. P., Lee, C., et al. (2010). Calcium carbonate saturation states in the waters of the Canadian Arctic Archipelago and the Labrador Sea. *Journal of Geophysical Research*, 115. https://doi.org/10.1029/2009JC005917 Azetsu-Scott, K., Petrie, B., Yeats, P., & Lee, C. (2012). Composition and fluxes of freshwater through Davis Strait using multiple chemical tracers. *Journal of Geophysical Research*, 117. https://doi.org/10.1029/2012JC008172

Ballinger, T., Hanna, E., Hall, R., Miller, J., Ribergaard, M., & Hoyer, J. (2018). Greenland coastal air temperatures linked to Baffin Bay and Greenland Sea ice conditions during autumn through regional blocking patterns. *Climate Dynamics*, 50, 83–100. https://doi.org/10.1007/s00382-017-3583-3

Bauer, M., Tselioudis, G., & Rossow, W. (2016). A new climatology for investigating storm influences in and on the extratropics. *Journal of Applied Meteorology and Climatology*, 55, 1287–1303. https://doi.org/10.1175/JAMC-D-15-0245.1

Cappelen, J. (Ed.). (2018). Greenland - DMI historical climate data collection 1784-2017. Technical Report 18-04. DMI.

Cuny, J., Rhines, P., & Kwok, R. (2005). Davis Strait volume, freshwater and heat fluxes. *Deep Sea Research*, 52, 519–542. https://doi.org/10.1016/j.dsr.2004.10.006

Curry, B., Lee, C. M., & Petrie, B. (2011). Volume, freshwater and heat fluxes through Davis Strait, 2004–05. Journal of Physical Oceanography, 41, 429–436. https://doi.org/10.1175/2010jpo4536.1

Curry, B., Lee, C. M., Petrie, B., Moritz, R., & Kwok, R. (2014). Multiyear volume, liquid freshwater and sea ice transports through Davis Strait, 2004–10. *Journal of Physical Oceanography*, 44, 1244–1266. https://doi.org/10.1175/jpo-d-13-0177.1

de Jong, M. F., Bower, A. S., & Furey, H. H. (2016). Seasonal and interannual variations of Irminger ring formation and boundary-interior heat exchange in FLAME. *Journal of Physical Oceanography*, 46, 1717–1734. https://doi.org/10.1175/JPO-D-15-0124.1

Fichefet, T., & Morales Maqueda, M. A. (1997). Sensitivity of a global sea ice model to the treatment of ice thermodynamics and dynamics. Journal of Geophysical Research, 102, 12609–12646. https://doi.org/10.1029/97jc00480

Foukal, N. P., & Lozier, M. S. (2017). Assessing variability in the size and strength of the North Atlantic subpolar gyre. *Journal of Geophysical Research*, 122, 6295–6308. https://doi.org/10.1002/2017JC012798

Gelaro, R., McCarty, W., Suárez, M. J., Todling, R., Molod, A., Takacs, L., et al. (2017). The modern-era retrospective analysis for research and applications, version 2 (MERRA-2). *Journal of Climate*, 30, 5419–5454. https://doi.org/10.1175/JCLI-D-16-0758.1

Gladish, C. V., Holland, D. M., & Lee, C. M. (2015). Oceanic boundary conditions for Jakobshavn Glacier. Part II: Provenance and sources of variability of Disko Bay and Illulissat icefjord waters, 1990–2011. *Journal of Physical Oceanography*, 45, 33–63. https://doi.org/10.1175/IPO-D-14-00451

Godfrey, J. S. (1989). A Sverdrup model of the depth-integrated flow for the world ocean allowing for island circulations. *Geophysical and Astrophysical Fluid Dynamics*, 45, 89–112. https://doi.org/10.1080/03091928908208894

Hanna, E., Cropper, T., Hall, R., & Cappelen, J. (2016). Greenland Blocking Index 1851–2015: A regional climate change signal. International Journal of Climatology, 36, 4847–4861. https://doi.org/10.1002/joc.4673

Hanna, E., Cropper, T., Jones, P., Scaife, A., & Allan, R. (2015). Recent seasonal asymmetric changes in the NAO (a marked summer decline and increased winter variability) and associated changes in the AO and Greenland Blocking Index. *International Journal of Climatology*, 35, 2540–2554. https://doi.org/10.1002/joc.4157

Hanna, E., Fettweis, X., Mernild, S., Cappelen, J., Ribergaard, M., Shuman, C., et al. (2014). Atmospheric and oceanic climate forcing of the exceptional Greenland ice sheet surface melt in summer 2012. *International Journal of Climatology*, 34, 1022–1037. https://doi.org/10.1002/joc.3743

Hersbach, H., Bell, B., Berrisford, P., Hirahara, S., Horányi, A., Muñoz-Sabater, J., et al. (2020). The ERA5 global reanalysis. *Quarterly Journal of the Royal Meteorological Society*, 146, 1999–2049. https://doi.org/10.1002/qj.3803

 $Hersbach,\,H.,\,\&\,\,Dee,\,D.\,\,J.\,\,E.\,\,N.\,\,(2016).\,\,ERA5\,\,reanalysis\,\,is\,\,in\,\,production.\,\,ECMWF\,\,Newsletter,\,147,\,5-6.$

Holland, D. M., Thomas, R. H., de Young, B., Ribergaard, M., & Lyberth, B. (2008). Acceleration of Jakobshavn Isbrae triggered by warm subsurface ocean waters. *Nature Geoscience*, 1, 659–664. https://doi.org/10.1038/ngeo316

Hu, X. (2020). ANHA12-EXH006. UAL Dataverse, V1. https://doi.org/10.7939/DVN/5G0NGP

Hu, X., Sun, J., Chan, T., & Myers, P. G. (2018). Thermodynamic and dynamic ice thickness contributions in the Canadian Arctic Archipelago in NEMO-LIM2 numerical simulations. *The Cryosphere*, 12, 1233–1247. https://doi.org/10.5194/tc-12-1233-2018

Joughin, I., Shean, D. E., Smith, B. E., & Floricioiu, D. (2020). A decade of variability of Jakobshavn Isbrae: Ocean temperatures pace speed through influence on melange rigidity. *The Cryosphere*, 14, 211–227. https://doi.org/10.5194/tc-14-211-2020

Joyce, T. M., & Proshutinsky, A. (2007). Greenland's island rule and the Arctic Ocean circulation. *Journal of Marine Research*, 65, 639–653. https://doi.org/10.1357/002224007783649439

Khazendar, A., Fenty, I. G., Carroll, D., Gardner, A., Lee, C. M., Fukumori, I., et al. (2019). Interruption of two decades of Jakobshavn Isbrae acceleration and thinning as regional ocean cools. *Nature Geoscience*, 12, 277–283. https://doi.org/10.1038/s41561-019-0329-3

Luo, H., Castelao, R. M., Rennermalm, A. K., Tedesco, M., Braco, A., Yager, P. L., & Mote, T. L. (2016). Oceanic transport of surface meltwater from the southern Greenland ice sheet. *Nature Geoscience*, 9, 528–532. https://doi.org/10.1038/NGEO2708

Madec, G. (2008). NEMO ocean engine. Technical Report Notes de Pole de modelisation (Vol. 27). Institut Pierre-Simon Palace (IPSL).

Manney, G., Santee, M. L., Rex, M., Livesey, N. J., Pitts, M. C., Veefkind, P., et al. (2011). Unprecedented Arctic ozone loss in 2011. *Nature*, 478, 469–475. https://doi.org/10.1038/nature10556

Melling, H., Agnew, T. A., Falkner, K. K., Greenberg, D. A., Lee, C. M., Münchow, A., et al. (2008). Fresh-water fluxes via Pacific and Arctic outflows across the Canadian Polar Shelf. In B. Dickson, J. Meincke, & P. Rhines (Eds.), Arctic-Subarctic Ocean Fluxes: Defining the role of the northern seas in climate (pp. 193–247). Springer. https://doi.org/10.1007/978-1-4020-6774-7_10

Moore, G., & Renfrew, I. (2011). Cold European winters: Interplay between the NAO and the East Atlantic mode. *Atmospheric Science Letters*, 13, 1–8. https://doi.org/10.1002/asl.356

Moore, G., Schweigher, A., Zhang, J., & Steele, M. (2018). What caused the remarkable February 2018 North Greenland polynya? *Geophysical Research Letters*, 45. https://doi.org/10.1029/2018GL080902

Mortensen, J., Bendtsen, J., Motyka, R. J., Lennert, K., Truffer, M., Fahnestock, M., & Rysgaard, S. (2013). On the seasonal freshwater stratification in the proximity of fast-flowing tidewater glaciers in a sub-Arctic sill fjord. *Journal of Geophysical Research*, 118, 1382–1395. https://doi.org/10.1002/jgrc.20134

Mortensen, J., Rysgaard, S., Arendt, K. E., Juul-Pedersen, T., Sogaard, D. J., Bendtsen, J., & Meire, L. (2018). Local coastal water masses control heat levels in a West Greenland tidewater outlet glacier fjord. *Journal of Geophysical Research*, 123, 8068–8083. https://doi.org/10.1029/JC014549

MYERS ET AL. 10 of 11



- Münchow, A. (2016). Volume and freshwater observations from Nares Strait to the west of Greenland at daily time scales from 2003 to 2009. Journal of Physical Oceanography, 46, 141–157. https://doi.org/10.1175/JPO-D-0093.1
- Myers, P. G., & Ribergaard, M. H. (2013). Warming of the polar water layer in Disko Bay and potential impact on Jakobshavn Isbrae. *Journal of Physical Oceanography*, 43, 2629–2640. https://doi.org/10.1175/JPO-D-12-051.1
- Peterson, I., Hamilton, J., Prinsenberg, S., & Pettipas, R. (2012). Wind-forcing of volume transport through Lancaster Sound. *Journal of Geophysical Research*, 117, C11018. https://doi.org/10.1029/2012JC/008140
- Rysgaard, S., Boone, W., Carlson, D., Sejr, M., Bendtsen, J., Juul-Pedersen, T., et al. (2020). An updated view of the water masses on the pan-West Greenland continental shelf and their link to proglacial fjords. *Journal of Geophysical Research*, 125. https://doi.org/10.1029/2019JC015564
- $Schulze\ Chretien,\ L.,\ \&\ Frajka-Williams,\ E.\ (2018).\ Wind-driven\ transport\ of\ fresh\ shelf\ water\ into\ the\ upper\ 30\ m\ of\ the\ Labrador\ Sea.$ $Ocean\ Science,\ 14.\ https://doi.org/10.5194/os-14-1247-2018$
- Smith, G. C., Roy, F., Mann, P., Dupont, F., Brasnett, B., Lemieux, J.-F., et al. (2014). A new atmospheric dataset for forcing ice-ocean models: Evaluation of reforecasts using the Canadian global deterministic prediction system. *Quarterly Journal of the Royal Meteorological Society*, 140, 881–894. https://doi.org/10.1002/qj.2194
- Straneo, F., & Heimbach, P. (2013). North Atlantic warming and the retreat of Greenland's outlet glaciers. *Nature*, 504, 36–43. https://doi.org/10.1038/nature12854
- Straneo, F., Sutherland, D. A., Holland, D., Gladish, C., Hamilton, G. S., Johnson, H. L., et al. (2012). Characteristics of ocean waters reaching Greenland's glaciers. *Annals of Glaciology*, 53. https://doi.org/10.3189/2012AoG60A059
- Tang, C., Ross, C., Yao, T., Petrie, B., DeTracey, B., & Dunlap, E. (2004). The circulation, water masses and circulation of Baffin Bay. *Progress in Oceanography*, 63, 183–228. https://doi.org/10.1016/j.pocean.2004.09.005
- Wood, M., Rignot, E., Fenty, I., Menemenlis, D., Morlighem, M., Moughinot, J., et al. (2018). Ocean-induced melt triggers glacier retreat in northwest Greenland. *Geophysical Research Letters*, 45, 8334–8342. https://doi.org/10.1029/2018GL078024

MYERS ET AL. 11 of 11